

## An exhaustive study of a coupling reagent (1-(3-dimethylaminopropyl) 3-ethylcarbodiimide hydrochloride) as corrosion inhibitor for steel

Shefali Dahiya<sup>1</sup>, Parmod Kumar<sup>1</sup>, Suman Lata\*<sup>1</sup>, Raman Kumar<sup>2</sup>, Naveen Dahiya<sup>3</sup> & Suman Ahlawat<sup>4</sup>

<sup>1</sup>Deenbandhu Chhotu Ram University of Science and Technology, Murthal, Haryana, India.

<sup>2</sup>University of Delhi, New Delhi, India.

<sup>3</sup>MSIT, Janak Puri, New Delhi, India.

<sup>4</sup>Department of Chemistry, MDU, Rohtak, India.

E-mail: sumanjakhar.chem@dcrustm.org

*Received 3 September 2015; accepted 6 February 2017*

The corrosion inhibition of mild steel in 0.5 M HCl by a coupling reagent, 1-(3-Dimethylaminopropyl) 3-ethylcarbodiimide hydrochloride (EDC), has been investigated by weight loss, electrochemical impedance spectroscopy (EIS), polarization technique, theoretical studies of quantum chemistry and scanning electron microscopy (SEM). Experimental results show that the reagent is an effective inhibitor for the corrosion of mild steel in acidic solution and it exhibited > 90% inhibition efficiency at low concentrations of the inhibitor. Potentiostatic polarization studies show that the studied compound is a mixed-type inhibitor. The results of EIS show that EDC inhibits corrosion of mild steel by adsorption mechanism. Surface morphology has been studied by SEM and the theoretical quantum calculations also are in agreement with the experimental results. The adsorption of inhibitor on the mild steel surface follow Langmuir adsorption isotherm. The thermodynamic parameters of corrosion process have also been calculated and discussed.

**Keywords:** Corrosion inhibition, Coupling reagent, Adsorption, Mild Steel, Thermodynamic properties

Corrosion is a fundamental process playing an insignificant role in economics and safety of metals. Among metals, Mild steel is a widely used commercial metal for fabrication, transportation and storage. The acid solutions are widely used in industries for acid pickling, industrial acid cleaning, acid descaling and oil well acidizing processes for mild steel and other alloys. Different concentrations of hydrochloric acid are most commonly used in these industries for this purpose. The most practical method for protection against corrosion of mild steel is the use of inhibitors, especially in acidic media and hence it leads the corrosion researchers to study the effect of various corrosion inhibitors on mild steel in hydrochloric acid environment.

The corrosion inhibitors have to be chemically stable providing higher protection, contributing to the increase in the corrosion inhibition efficiency<sup>1</sup>. The most common types of corrosion inhibitors for metals and their alloys act through adsorption inhibitors<sup>2</sup>. As the strong activity of acid solutions towards metal corrosion and its dissolution the adsorption inhibitors are used to inhibit the metal corrosion. The effect of

inhibitors adsorbed on metallic surface in acid solutions, slows down the anodic dissolution reactions as well as the cathodic processes occurring on the metal and it may control corrosion due to the formation of a barrier for further diffusion or by means of the blockage of the reaction sites<sup>2,3</sup>. These adsorption inhibitors are generally inorganic compounds like chromates, phosphates, molybdates, etc. and organic compounds containing N, O, S as heteroatoms or structures containing  $\pi$  electrons in their molecules<sup>4-6</sup>. The extent of adsorption also depends on the nature of the metal surface as well as the medium. The organic molecule acting as inhibitor, either forms a protective layer that prevents diffusion of the chemical species involved in the ionization of the metal or interacts with metals and retards the corrosion reaction. In fact, it is not possible to assign a single general mechanism of action to an inhibitor because the factors like concentration of inhibitor, pH and temperature of the solution, nature of the anion of the acid, nature of active centers of the inhibiting compound and the nature of the alloy may play a vigorous role. The mechanism of action of inhibitors

with the same functional groups may also vary with factors such as the effect of molecular structure, on the electron density of the functional group and the size of the aromatic and aliphatic portions of the molecule<sup>6,7</sup>. Adsorption of these organic inhibitors is achieved from interactions between metal (lowest unoccupied molecular orbital – LUMO) and non-participant electrons of heteroatoms or  $\pi$  electrons of the inhibiting compound (highest occupied molecular orbital – HOMO)<sup>8</sup>. The low energy gap between the two orbitals (LUMO and HOMO) facilitates the extent of interaction between the metal and the inhibitor and hence may show a good adsorption.

The use of conventional organic compounds as adsorption inhibitors have been questioned due to their multiple hazardous effects for the sake of maintaining the ecological balance. Thus, the development of non-toxic, biodegradable and eco-friendly compounds as corrosion inhibitors is in great demand increasing the passion among corrosion researchers of the day<sup>9</sup>.

The present research work deals with the study of biochemically active organic compound, EDC, which is a coupling reagent, involved in protein synthesis (Fig 1).

## Experimental Section

### Material

Commercial mild steel sheets of percentage composition 0.14 C, 0.03 Si, 0.032 Mn, 0.05 S, 0.20 P, 0.01 Ni, 0.01 Cu, 0.01 Cr and balanced Fe were used. The electrolyte solution, 0.5 M HCl, was prepared from analytical grade HCl using double distilled water. The inhibitor used is a coupling reagent. (1-(3-Dimethylaminopropyl) 3-ethylcarbodiimide hydrochloride) with molecular formula  $C_8N_3H_{17}$  and molecular weight 191.7g.

### Gravimetric analysis

The mild steel (MS) specimens used had a rectangular shape of (3 cm  $\times$  1.5 cm  $\times$  0.028 cm) were abraded with series of SiC paper (600, 800, 1000 and 1200 grades) and then washed with distilled water and followed by washing with acetone. After weighing accurately (citizen scale CX230), the specimens were immersed in conical flask containing 200 mL of 0.5

M HCl in the absence and presence of different concentrations (200 ppm, 400 ppm, 800 ppm and 1000 ppm) of the inhibitor. Each experiment was performed in duplicate in freshly prepared solution and the temperature was thermostatically controlled at 303-333K in thermostat for 4 h. Then, the specimens were taken out, washed thoroughly to remove the corrosion product, dried and weighed again. The corrosion rate (in mpy) in absence and presence of inhibitor was calculated.

### Electrochemical analysis

The electrochemical analysis was carried out in a conventional three-electrode cell using CHI760C analyser. A platinum foil was used as counter electrode with a saturated calomel electrode (SCE) coupled to a fine Luggin capillary as reference electrode and the working electrode was a 1cm<sup>2</sup> cut from the MS embedded in epoxy resin of polytetrafluoroethylene (PTFE).

### Polarization measurements

For polarization experiments, Tafel polarization curves were obtained by changing the electrode potential automatically from -500 to +500 mV at open circuit potential with a scan rate of 1 mVs<sup>-1</sup>. Stern-Geary method<sup>10</sup> was used for determining corrosion current by extrapolation of anodic and cathodic Tafel lines to a point which gives  $\log i_{\text{corr}}$  and the corresponding corrosion potential ( $E_{\text{corr}}$ ) for blank medium and different inhibitor's concentration.

### Impedance measurements

EIS measurements were carried out on the analyser in frequency range of  $1.0 \times 10^5$  - 1.0 Hz with the AC signal 5 mV peak-to-peak at open circuit potential. The same three electrode cell was maintained for EIS studies. The main parameters deduced from the analysis of Nyquist and Bode plots are the resistance of charge transfer  $R_{\text{ct}}$  (diameter of high frequency loop) and the capacity of double layer  $C_{\text{dl}}$ . The electrode potential was allowed to stabilize 4 h before starting the measurements. All the experiments were conducted at 303K  $\pm$  1.

### Quantum chemical study

The quantum chemical studies were performed for the present system by using AM1 (Austin Model1), a semi empirical method based on the neglect of differential diatomic overlap approximation. The quantum parameters were calculated using HyperChem professional 8.0 package (Hypercube

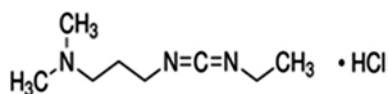


Fig 1 — Structure of EDC

Inc., USA). The technique was studied to correlate the various parameters and their results with the studied experimental data.

**Scanning electron microscopy (SEM)**

The MS specimens were immersed in blank (0.5 M HCl) solution and solutions having inhibitor concentration of 1000 ppm for 4 h. The coupons were immersed for 4 h duration at 303K temperature. The coupons were thoroughly polished using range of emery papers, washed and dried in acetone, similar to weight loss experiment. After the completion of 4 h the coupons were rubbed to scale off the corroded layer and then again washed and dried. SEM studies were performed using Model Zeiss Ultra 55 at 3kV.

**Results and Discussion**

**Gravimetric analysis**

The gravimetric analysis is performed on the basis weight loss observed in absence and presence of EDC<sup>11</sup>. The inhibition efficiency (IE%) of inhibitor on the corrosion of MS was calculated as follows (Eq. 1),

$$I.E\% = \frac{CR - CR_{inh}}{CR_{inh}} \times 100 \quad \dots (1)$$

where, CR and CR<sub>inh</sub> are the corrosion rates of mild steel in the absence and presence of the inhibitor, respectively.

The corrosion rate (CR) tabulated in Table 1. in mpy was calculated from the following equation (Eq. 2),

$$CR = \frac{534 \times W}{DA t} \quad \dots (2)$$

where, W is the average weight loss of mild steel specimens (mg), A is total area of one MS specimen in cm<sup>2</sup>, t is the immersion time (4 h) and D is density of mild steel (7.86 gcm<sup>-3</sup>). The technique suggested that the increase in the inhibitor concentration results

in the increase in inhibition efficiency and decrease in corrosion rate. The study also suggested the optimum concentration of inhibition is 800 ppm, might be due to the adsorption behavior of the inhibitor, as discussed later. The inhibitor shows remarkable efficiency at lower studied concentrations except in the last studied. The efficiency remains almost same and often decreases too. This is well depicted from the Fig. 2 showing change in inhibition efficiency with increasing concentration.

**Polarization measurement**

Potentiostatic anodic and cathodic polarization plots for MS specimens in 0.5 M HCl solution in the absence and presence of varying concentrations of inhibitor were plotted at 303-333K (Fig. 3). The plots depict the electrochemical kinetic parameters such as corrosion current density (I<sub>corr</sub>), corrosion potential (E<sub>corr</sub>), cathodic and anodic Tafel slopes (β<sub>c</sub>) and (β<sub>a</sub>) respectively, given in Table 2. The i<sub>corr</sub> from the experimental data is used for calculation of inhibition efficiency and surface coverage (θ) as in Eq. 3<sup>12</sup>:

$$\% IE = \theta \times 100 = [1 - (i_{corr} / i_{corr}^0)] \times 100 \quad \dots (3)$$

where, i<sup>0</sup><sub>corr</sub> and i<sub>corr</sub> are the corrosion current densities in the absence and presence of inhibitor, respectively. The increasing efficiencies with EDC concentrations suggest that the inhibition is increasing while with increase in temperatures, the efficiency decreases indicating the desorption of inhibitor at higher temperatures. Also the gravimetric results of optimum concentration are strengthened showing maximum inhibition at 800 ppm concentration of EDC in 0.5M HCl. With the increase in the inhibitor concentration the decrease in current density suggests that due to the

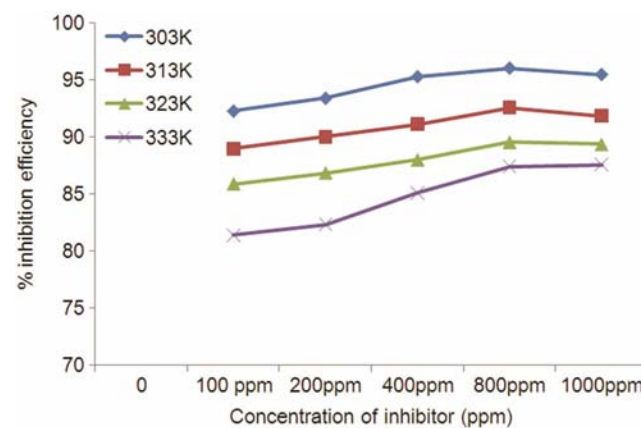


Fig. 2 — Plot between inhibition efficiency and concentrations (200 ppm, 400 ppm, 800 ppm, 1000 ppm) of EDC at different temperature (303K - 333K) from gravimetric data.

Table 1 — Corrosion rates of MS in 0.5 M HCl in absence and presence of EDC concentrations

	Corrosion rate (mpy × 10 <sup>3</sup> )			
	303K	313K	323K	333K
Blank	313.654	331.931	351.387	383.814
100 ppm	24.173	36.554	43.039	71.339
200ppm	20.635	32.427	40.091	67.801
400ppm	14.739	28.889	36.553	57.189
800ppm	12.381	24.173	31.837	40.681
1000ppm	14.15	26.531	32.426	47.756

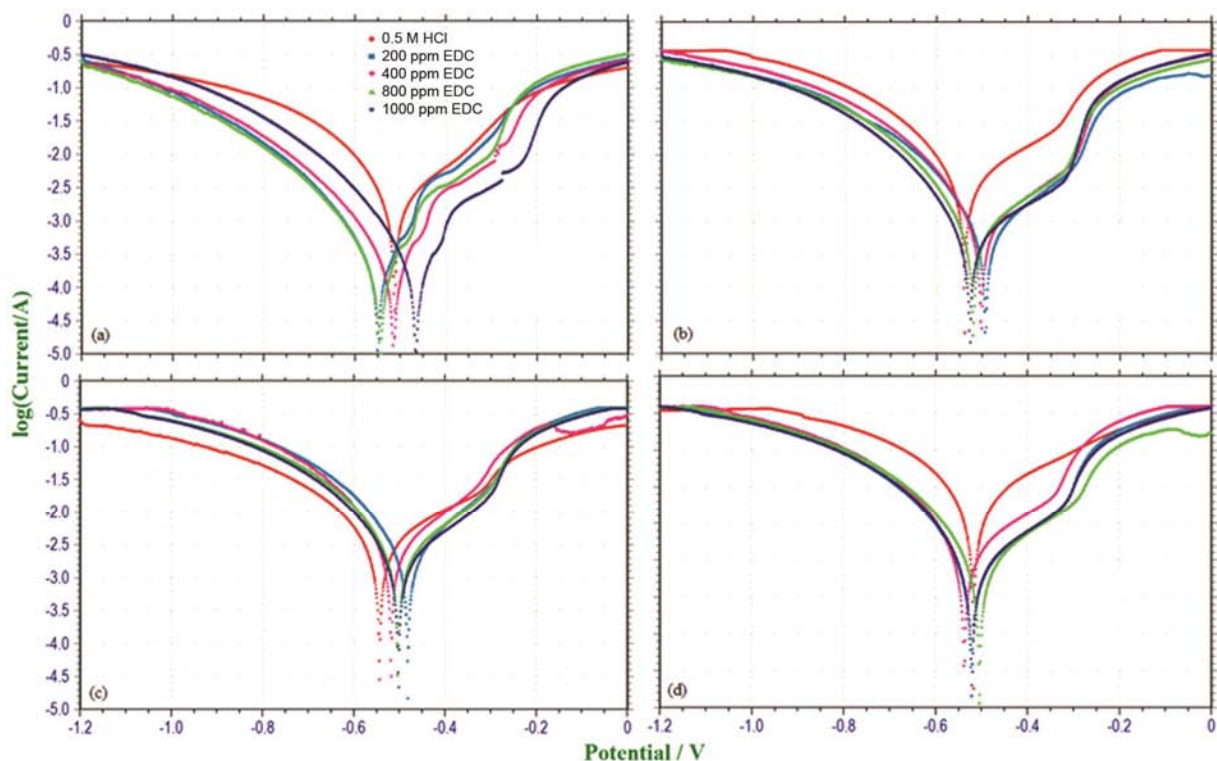


Fig 3 — Tafel curves of EDC inhibitor at concentrations (200 ppm, 400 ppm, 800 ppm and 1000 ppm) in 0.5 M HCl at (a)303K (b)313K (c)323K (d)333K.

Table 2 — Polarization data of EDC at various concentration and temperature for MS in 0.5 M HCl.

Temperature K	Inhibitor Conc. (ppm)	$-E_{\text{corr}}$ (mV)	$\beta_a$ (mV/dec)	$\beta_c$ (mV/dec)	$i_{\text{corr}}$ (mA/cm <sup>2</sup> )	I.E.(%)	$\Theta$	
303 -	200	0.513	131.87	192.23	2.218	-	-	
	400	0.515	103.21	165.53	0.1579	92.88	0.9288	
	800	0.545	106.53	174.09	0.1255	94.34	0.9434	
	1000		0.466	97.96	187.97	0.1833	95.63	0.9563
			0.549	103.55	223.61	0.1625	94.45	0.9445
313 -	200	0.539	131.97	205.67	7.95	-	-	
	400	0.503	117.71	206.01	0.859	89.19	0.8919	
	800	0.521	112.72	227.01	0.734	90.76	0.9076	
	1000		0.528	115.11	228.67	0.5958	92.51	0.9251
			0.493	108.62	219.01	0.6891	91.33	0.9133
323 -	200	0.507	196.15	205.97	17.41	-	-	
	400	0.518	128.43	197.08	3.011	82.7	0.827	
	800	0.504	130.45	196.12	2.19	87.42	0.8742	
	1000		0.502	137.12	203.09	1.926	88.93	0.8893
			0.481	119.46	205.38	2.232	87.17	0.8717
333 -	200	0.517	170.13	213.72	19.08	-	-	
	400	0.538	133.28	225.12	4.523	76.29	0.7629	
	800	0.505	127.21	223.16	3.122	83.63	0.8363	
	1000		0.521	126.82	226.04	2.889	84.85	0.8485
			0.522	125.18	214.96	2.753	85.57	0.8557

anodic dissolution, the hydrogen evolution is retarded. No remarkable shift in  $E_{\text{corr}}$  values was observed in the absence and presence of different concentrations of the inhibitors, signifying that the inhibitor seems to behave as mixed-type inhibitor.

#### Electrochemical impedance spectroscopy (EIS)

The Nyquist plots obtained from EIS measurements and the results are tabulated in Table 3. It is clear from the plots that the impedance response of MS in uninhibited 0.5 M HCl has significantly

improved after the addition of inhibitor into the corrosive solutions. The charge-transfer resistance ( $R_{ct}$ ) values were calculated from the difference in impedance at lower and higher frequencies<sup>13</sup>. The double layer capacitance ( $C_{dl}$ ) is then calculated using Eq. 4 which is defined as:

$$C_{dl} = 1 / (2 \pi f_{max} R_{ct}) \quad \dots (4)$$

where,  $f_{max}$  is the maximum frequency.

Nyquist plots size increased with the inhibitor concentration suggested that there is increase in  $R_{ct}$  values and lowering in then calculated  $C_{dl}$ .

The inhibition efficiencies and the surface coverage ( $\theta$ ) obtained from the impedance measurements were calculated from Eq. 5 :

$$\%IE = \theta \times 100 = [1 - (R_{ct}^0 / R_{ct})] \times 100 \quad \dots (5)$$

where  $R_{ct}^0$  and  $R_{ct}$  are the charge transfer resistance in the absence and presence of inhibitor, respectively. EIS studies indicated that EDC is a good inhibitor at 303K with inhibition efficiency of > 93% (Table 3). The inhibition is due to the formation of inhibitive film over the MS surface that was strengthened by addition of more of inhibitor and hence showing the increase in charge transfer process mainly controlling the corrosion of MS.

The decrease in  $C_{dl}$  is supposed to be due to the rising surface coverage by the inhibitor molecules and the decrease in local dielectric constant. The relationship between  $C_{dl}$  values and the thickness of the protective layer,  $\delta_{org}$ , is given as<sup>14</sup> in Eq. 6

$$\delta_{org} = \frac{\epsilon_0 \epsilon_r}{C_{dl}} \quad \dots (6)$$

where ,  $\epsilon_0$  is the dielectric constant and  $\epsilon_r$  is the relative dielectric constant.

The increase in the thickness of the electrical double layer expected to decrease in its  $C_{dl}$  values, suggesting that the EDC molecule acts by adsorption forming the interface between MS and 0.5 M HCl medium. As a result, the decrease in  $C_{dl}$  values may

be due to the gradual replacement of water molecules by the adsorption of the organic molecules on the metal surface and thereby decreasing the extent of metal dissolution in the acidic medium.

**Scanning Electron Microscopy (SEM)**

SEM images of the MS in the absence and presence of inhibitor are shown in Fig. 4(a) and Fig. 4(b), respectively. The surface morphology of the inhibited metal surface is smoother than the uninhibited surface representing a protective layer of adsorbed inhibitor preventing corrosion due to acid attack on the mild steel surface. The smoothness of the MS surface in the presence of EDC is owing to the barrier of the protective film over the metal surface.

**Quantum chemical analysis**

Quantum chemical and theoretical study of the compound used as corrosion inhibitor are studied,

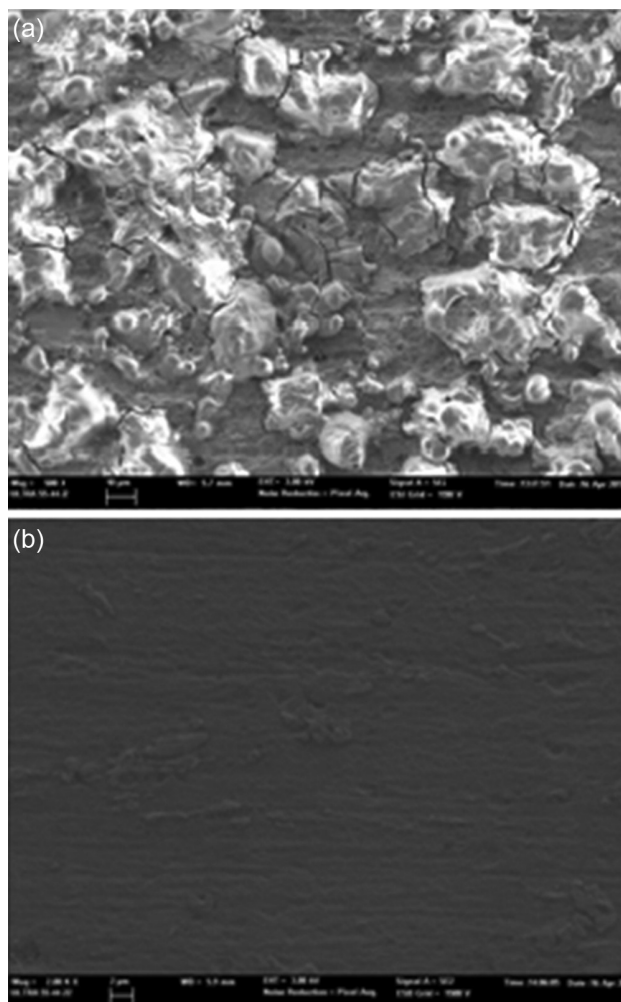


Fig 4 — Scanning electron micrographs of the mild steel surface after 4 h immersion at 303 K in (a) blank ,and (b) 1000 ppm of EDC.

Table 3 — Electrochemical Impedance values with and without EDC concentrations in 0.5 M HCl at 303K.

Inhibitor Conc. (ppm)	$f_{max}$ value	$R_{ct}$ ( $\Omega \text{ cm}^2$ )	$C_{dl}$ ( $\text{Fcm}^{-2}$ )	% I.E
0	5.42	14.114	2.082	0
200	32.86	214.018	2.26E-05	93.40
400	42.98	219.955	1.68E-05	93.58
800	44.52	221.571	1.61E-05	93.63
1000	43.69	219.965	1.66E-05	93.58

used to determine the relationship between the molecular structure of the compound and its experimental corrosion inhibition efficiencies<sup>15</sup>. The quantum chemical parameters, namely  $E_{\text{HOMO}}$  (highest occupied molecular orbital energy),  $E_{\text{LUMO}}$  (lowest unoccupied molecular orbital energy), the energy difference ( $\Delta E$ ) between  $E_{\text{HOMO}}$  and  $E_{\text{LUMO}}$ , dipole moment ( $\mu$ ), electron affinity ( $A$ ), ionization potential ( $I$ ), the absolute electronegativity ( $\chi$ ), absolute hardness ( $\eta$ ), softness ( $\sigma$ ), the Mulliken charges and the fraction of electrons ( $\Delta N$ ) transfer from EDC to iron, were determined and correlated with the experimental data. The aim of the study is to find good theoretical parameters to determine the inhibition property of the inhibitor and the correlation between the inhibition efficiency and the electronic properties. Following are the various studied quantum parameters for the inhibitor in Table 4.

Values of  $\chi_{\text{inh}}$ ,  $\sigma_{\text{inh}}$  and  $\eta_{\text{inh}}$  were calculated by using the values of  $I$  and  $A$  obtained from quantum chemical calculation, where,  $I = -E_{\text{HOMO}}$  and  $A = -E_{\text{LUMO}}$

$$\chi = (I+A)/2 \quad \dots (7)$$

$$\eta = (I-A)/2 \quad \dots (8)$$

$$\sigma = 1/\eta \quad \dots (9)$$

and  $\Delta N$ , the fraction of electrons transferred from inhibitor to the iron molecule, was calculated, using a theoretical  $\chi_{\text{Fe}}$  value of 7 eV/mol and  $\eta_{\text{Fe}}$  value of 0 eV/mol for iron atom in the equation as below:

$$\Delta N = (\chi_{\text{Fe}} - \chi_{\text{inh}}) / [2 (\eta_{\text{Fe}} + \eta_{\text{inh}})] \quad \dots (10)$$

The calculated  $\Delta N$  value of the inhibitor showed inhibition effect of EDC due to the fraction of electron donated to the LUMO of the iron (acceptor)

Table 4 — Quantum chemical parameters derived for EDC calculated with AM1.

Quantum parameters	
Total energy(kJ/mol)	-181229.937
Heat of formation (kJ/mol)	154.0046275
Dipole moment (D)	1.669
$E_{\text{HOMO}}$ (eV)	-9.191854
$E_{\text{LUMO}}$ (eV)	0.929248
$\Delta E$ ( $E_{\text{LUMO}} - E_{\text{HOMO}}$ ) (eV)	10.145
$I$ (Ionization potential)	9.191854
$A$ (Electron affinity)	-0.929248
$H$ (Hardness)	5.072
$\sigma$ (Softness)	0.1971
$\chi$ (Electronegativity)	4.344
$\Delta N$ (Fraction of electrons)	0.2618

from the HOMO of the inhibitor (donor). The compound is bound to the metal surface and thus is expected to form inhibition adsorption layer protecting the metal surface from corrosion. According to Lukovits's study<sup>16</sup>, upto  $\Delta N < 3.6$ , the inhibition efficiency increases with increasing electron-donating capability at the metal surface. The  $\Delta N$  value in the present study is 0.26 which suggests the adsorption is also due to this transfer of electrons to the metal surface and certainly should increase with increasing inhibitor concentration, the similar result was obtained from the experimental data where inhibition efficiency increases with the increase in concentration. The quantum results also strengthen the chemical adsorption along with the physical one.

Mulliken population analysis (Fig. 5a) is used to calculate approximately the adsorption centers of the inhibitor<sup>17</sup>, in addition to the electron charge distribution over the complete molecule (Fig. 5b). The atom with greater negative charge is more likely the donation center of the inhibitor which can donate its electron density to the metal surface *via* a donor-acceptor type reaction. The Table 5 shows that all the

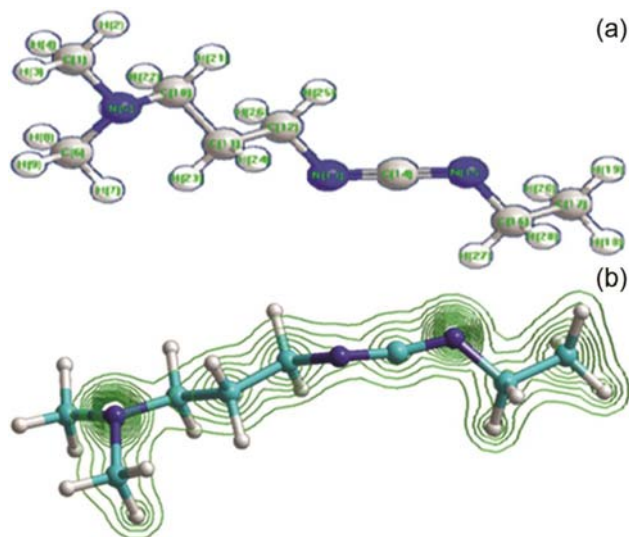


Fig. 5 (a) — Optimized structure of the inhibitor and (b) Electron density, of EDC using AM1.

Table 5 — Calculated Mulliken atomic charges (For atoms with more electron density) for EDC using AM1

Atom No.	Type	Charge	Atom No.	Type	Charge
1	C	-0.123	13	N	-0.213
5	N	-0.261	14	C	0.104
6	C	-0.119	15	N	-0.212
10	C	-0.068	16	C	-0.043
11	C	-0.158	17	C	-0.208
12	C	-0.042			

nitrogen atoms have high negative charge densities suggesting that the most apparent reactive centers for the adsorption of the inhibitor on mild steel surface is located on these atoms.

**Adsorption isotherms**

Basic information on the interaction between the surface of MS and inhibitor can be determined from several adsorption isotherms. The commonly used adsorption isotherms are Temkin, Frumkin, Langmuir and Flory – Huggins isotherm. The interactions of the inhibitor and the mild steel surface can be examined by the adsorption isotherm. The degree of surface coverage ( $\theta$ ) values for various concentrations ( $c$ ) of the inhibitors in the solution have been estimated from the polarization measurements. A straight line with linear correlation coefficient ( $R^2$ ) is almost equal to 1.0, was obtained on plotting  $C/\theta$  versus  $C$  at all studied different temperatures as shown in Fig. 6, indicating that adsorption of the inhibitor on the MS obeys the Langmuir adsorption isotherm. The linear relationships of  $C/\theta$  versus  $C$  suggest that the adsorption obeyed the Langmuir adsorption isotherm. This isotherm can be represented as Eq. 11<sup>18</sup>:

$$C/\theta = 1/K_{ads} + C \quad \dots (11)$$

Langmuir adsorption isotherm assumes that the adsorption of organic molecule on the adsorbent is monolayer and occurs through a physical adsorption mechanism<sup>19</sup>.

To determine the spontaneity of the corrosion reaction, the Free energy of adsorption ( $\Delta G$ ) for the reaction was calculated, using equations below (Eq. 12 and Eq. 13) :

$$\Delta G^\circ = -RT \ln 55.5 K_p \quad \dots (12)$$

$$\Delta G^\circ = -2.303RT \log 55.5 K_p \quad \dots (13)$$

where,  $K_p$  is the rate constant obtained graphically,  $R$  is a universal gas constant and  $T$  is temperature in kelvin. As the  $\Delta G^\circ$  values are greater than  $-20$  kJ/mol the adsorption is physical moving towards the chemical adsorption. The negative values of  $\Delta G^\circ_{ads}$  indicated the spontaneous adsorption of inhibitor on surface of mild steel [20]. The order of  $\Delta G^\circ$  value (Table 6) confirms that inhibition reaction at lower temp is more spontaneous shifting towards less spontaneity at 333K.

The corrosion process can be considered as an Arrhenius-type reaction, and its rate is given by Eq. 14:

$$I_{corr} = k \exp\left(-\frac{E_a}{RT}\right) \quad \dots (14)$$

where,  $k$  is the Arrhenius pre-exponential constant, and  $E_a$  is the activation energy for the corrosion process. The medium without EDC is showing 29.01 kJ/mol of activation energy which shoots upto 41.51 kJ/mol at 200 ppm. This change in activation energy ( $E_a$ ) with EDC concentration depicts towards the increase in the height of energy barrier, for the formation of the inhibiting complex that retards the corrosion reaction in 0.5 M HCl medium. With the increasing concentrations i.e. 400 ppm, 800 ppm and 1000 ppm.  $E_a$  value is observed to decrease gradually as 39.4 kJ/mol, 34.6 kJ/mol and 35.5 kJ/mol, respectively. The trend in activation energy clearly depicts the increase in inhibition efficiency at various concentrations, and maximum at 800 ppm. The optimum concentration for highest efficiency is also supported by the lowest calculated activation energy. This discussion, also, highlights greater adsorption at 800 ppm of EDC in 0.5 M HCl.

$$\log K = \frac{-\Delta H^*_{ads}}{2.303RT} + \frac{\Delta S^*_{ads}}{2.303R} \quad \dots (15)$$

A plot of  $\log K$  against  $1/T$  gives straight lines with slopes of  $\frac{-\Delta H^*_{ads}}{2.303}$  and intercepts of  $\frac{\Delta S^*_{ads}}{2.303R}$ . Using the eq. 15 the negative values of  $\Delta S^*$  ( $-112.8$  J/K/mol) and  $\Delta H^*$  ( $-46.05$  kJ/mol) indicates that the process of

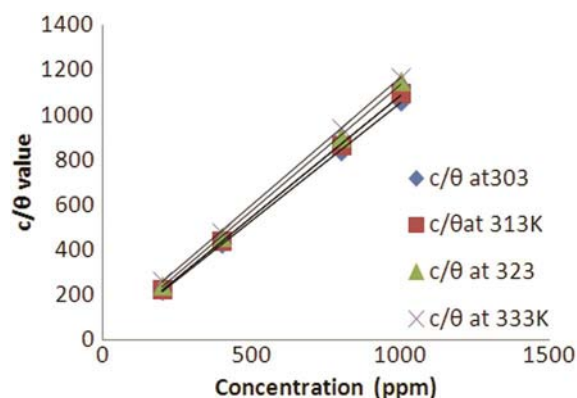


Fig. 6 — Langmuir adsorption isotherm of EDC on MS surface in 0.5 M HCl at different

Table 6 — Free energy change of adsorption of EDC in 0.5 M HCl.

Temperature (K)	lnK (constant)	$-\Delta G$ (kJ/mol)
303	5.563169	24.13
313	5.030185	23.54
323	4.534991	22.96
333	3.515464	20.85

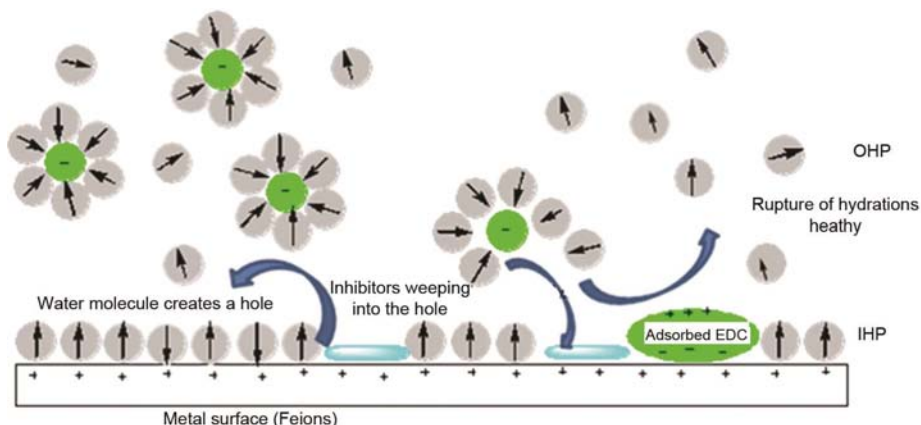
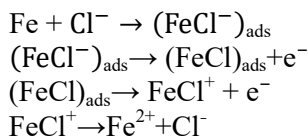


Fig. 7 — Mechanism of inhibition of MS surface by EDC in 0.5 M HCl

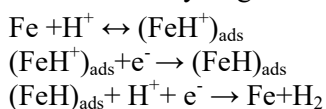
adsorption is exothermic and spontaneous<sup>21</sup>. During this process, the involved particles (MS surface, EDC and water molecules) break old attachments and make new ones resulting into change in enthalpy as well as exchange of freedoms and restrictions means change of entropy.

#### Mechanism of Inhibition

In HCl solution, metal undergoes two types of reactions, anodic and cathodic. The anodic reaction gives  $\text{Fe}^{++}$  and cathodic shows the liberation of the hydrogen gas<sup>22</sup>.

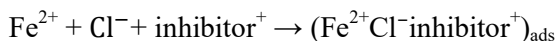


The cathodic hydrogen evolution mechanism is:



The adsorption of organic inhibitor molecules is often a displacement reaction involving removal of adsorbed water molecules from the metal surface.

In the presence of inhibitor, the reaction followed can be



The Metal –Inhibitor –Chloride ion complex may be formed and gets adsorbed over the mild steel surface that acts like a barrier in the acid attack and consequently, slows down the corrosion process. As the free-energy change is negative, the inhibitor may depart from OHP to IHP and consequently to the metal surface<sup>4</sup>. First, a vacancy from IHP may be

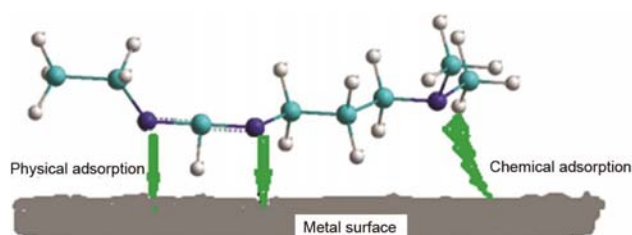


Fig. 8 — Modes of adsorption of EDC on MS surface.

swept free of water molecules in order to make a room for the inhibitor whereas the inhibitor gets rid off part of its solvent sheath simultaneously and then jumps into the vacancy, showing contact adsorption as shown in Fig. 7.

$\text{Organic inhibitor}_{(\text{solution})} + n\text{H}_2\text{O}_{(\text{adsorption})} \rightarrow \text{Organic inhibitor}_{(\text{adsorption})} + n\text{H}_2\text{O}_{(\text{solution})}$  where  $n$  water molecules on the electrode have to be displaced in order to incorporate one organic inhibitor molecule.

The exact nature of the interactions between a metal surface and the inhibitor molecule towards the given metal depends on the relative adsorbilities of the particular groups present in the inhibitor<sup>9</sup>. Fig. 8 indicates that, in addition to the physical adsorption (as evidenced by the results of adsorption study), chemical adsorption may also take place to some extent as the values of  $\Delta G^\circ$  given in Table 6 are shifting towards more negative side.

#### Conclusion

- The inhibition effect of EDC as a corrosion inhibitor was evaluated for the protection of mild steel corrosion in 0.5 M HCl solution using weight loss method, linear polarization, electrochemical impedance spectroscopy, scanning electron microscopic studies and quantum chemical study too.



- It was found that the studied compound can be exploited as an effective inhibitor for corrosion in the present system.
- The inhibition efficiency of the inhibitor gets enhanced with increase in its concentration but shows downfall with increasing temperature.
- Adsorption study showed that the inhibition mechanism obeyed Langmuir adsorption isotherm.
- The Tafel plots have shown that the EDC acted as mixed type inhibitor.
- The results of the gravimetric analysis, electrochemical polarizations, and EIS were in very good agreement .
- Photographs by scanning electron microscopy (SEM) have clearly shown that the rough surface of mild steel specimen has been improved, quite considerably in the presence of EDC.
- The quantum chemical data also supported the experimental output.

#### Acknowledgement

The authors are grateful to Prof. Gurmeet Singh, University of Delhi, Delhi, India for providing the facilities of electrochemical studies, as well as Professor B.Mari, Polytechnique University of Valencia, Spain , for providing the SEM facilities and Department of Chemistry, Deenbandhu Chhotu Ram University of Science and Technology, Murthal, Sonapat Haryana, for providing necessary facilities and encouragement.

#### References

- 1 Popova A, *Corros Sci*, 49 (2007) 2144.
- 2 Jauhari S, Mistry B M, Patel N S & Patel M J, *Res Chem Intermed*, 37 (2011) 659.
- 3 Silva A B, Agostinho S M L, Barcia O E , Cordeiro G G O & D'Elia E, *Corros Sci*, 48 (2006) 3668.
- 4 Bockris John O'M & Reddy A K N, *Electrochem Corr Sci*, (Kluwer Academic, New York ), 2004.
- 5 Bahrami M J, Hosseini S M A & Pilvar P, *Corros Sci*, 52 (2010) 2793.
- 6 Eddy N O & Ebenso E E, *African J Pure App Chem*, 2 (2008) 46.
- 7 Ai J Z, Guo X P, Qu J E, Chen Z Y & Zheng J S, *Colloids Surf A: Physicochem Eng Aspects*, 281 (2006) 147.
- 8 Khalil N, *Electrochim Acta*, 48 (2003) 2635.
- 9 Bobina M, Kellenberger A, Millet J P ,Muntean C & Vaszilescu N, *Corros Sci*, 69 (2013), 389.
- 10 Lata S & Choudhary R S, *Indian J Chem Technol*, 15 (2008) 364.
- 11 Iloamae I M, Onuegbu T U, Ajiwe V I E & Umeobika U C, *IJPAES*, 2 (2012) 56.
- 12 Nahlé A, IAbu-Abdoun I & Abdel-Rahman I, *Anti-Corros Methods Mater*, 54 (2007) 244.
- 13 Ahamad I, Prasad R & Quraishi M A, *Corros Sci*, 52 (2010) 3033.
- 14 Kaplan L G, *Intermolecular interactions : Physical picture, computational methods and model potentials* (Hoboken; Wiley, New Jersey) 2006.
- 15 Hong Ju, Zhen-Peng Kai & Yan Li, *Corro Sci*, 50 (2008) 865 .
- 16 Lukovits I, Kalman E & Zucchi F, *Corrosion*, 57 (2001) 3.
- 17 Jua H, Kaic Z & Yan Li, *Corros Sci*, 50 (2000) 865.
- 18 Popova A, Christov M & Zwetanova A, *Corros Sci*, 49 (2007) 2131.
- 19 Popova A, Christov M & Deligeorgiev T, *Corrosion* , 59 (2003) 756.
- 20 Samide A, Tutunaru & Negrila, *Chem Biochem Eng*, 25(2011) 299.
- 21 Safak S, Duran B, Yurt A & Turkoglu G, *Corros Sci*, 54 (2012) 251.
- 22 Eddy N O & Odoemelam S A, *Adv Nat Appl Sci*, 2 (2008) 225.